The International Journal of Advanced Manufacturing Technology (2021) 115:1671–1681
https://doi.org/10.1007/s00170-021-07237-6

ORIGINAL ARTICLE

Effect of heat treatment on microstructure and tribological behavior of friction stir processed Al_2O_3-reinforced AA2024-T351 matrix

Adel Haddad[1] · Abdessabour Benamor[1] · Nabil Chiker[1] · Youcef Hadji[1] · Mustapha Temmar[2] · Maamar Hakem[3] · Riad Badji[3] · Said Abdi[4] · Mohamed Hadji[1,3]

Received: 4 December 2020 / Accepted: 4 May 2021 / Published online: 16 May 2021

Abstract

In the present work, 2024-T351 Al alloy reinforced with alumina particulates (Al_2O_{3p}) was elaborated using friction stir processing (FSP). The effect of solution heat treatment followed by subsequent aging on microstructure, hardness, and tribological behavior is discussed. It was noticed that the hardness of the as-FSPed 2024-T351/Al_2O_{3p} was slightly enhanced in comparison to the as-received AA2024-T351 material, whereas the resulting wear resistance was remarkably improved. After heat treatment process, the composite volume increased, and swelling and pores were created at the processed area. The heat treatment caused a degradation in wear resistance compared to as-FSPed composites. The precipitation mechanism changed for AA2024/Al_2O_{3p}; reactions occurred at grain boundaries between Al_2O_3 and Cu or Mg, causing their depletion from the Al matrix. Intriguingly, the precipitation mode in heat-affected zone of the matrix also changed to grain boundary precipitation.

Keywords Friction stir processing · Metal matrix composites · Wear · Friction

1 Introduction

Alumina particles (Al_2O_{3p}) have been widely used as reinforcement particulates in an aluminum matrix, due to its low cost, availability, and wide range of commercial grades. Aluminum reinforced with Al_2O_{3p} proved their performance over unreinforced Al alloy; they are harder, stronger, tougher, and more wear-resistant [1–4]. These Al matrix composites (AMCs) are manufactured through different processes such as stir casting [5], infiltration [6], and squeeze casting filtration [7]. Even though these processes gained much attention due to their economic benefit, many limitations have been reported. Particle agglomeration and clustering, gravity segregation in case of nanoparticle-reinforced composites, and interfacial reactions between Al_2O_3 particles with molten Al have been the major issues [8]. Al_2O_3 is stable in most Al alloys except for Mg containing Al Alloys, and it may form spinel phase Al_2MgO_4 or Cu_2MgO_4 [8–12]. To overcome these issues, rheocasting, semisolid state processing, and powder metallurgy were used; thus, particle clustering was avoided, and interfacial reactions were minimized [13].

Friction stir processing (FSP), one of the solid state processing techniques, is the most industrially feasible process for bulk products used for many technologies such as surface modification, grain refinement, and surface composite manufacturing [14, 15]. When AMCs are processed by FSP, many issues could be solved such as particle clustering and interfacial reactions occurring at particle/matrix interface.

The incorporation of Al_2O_{3p} into the AA2024 matrix using FSP enhances the mechanical properties and wear resistance [16–18]. Several research works dealt with the effect of post-processing heat treatment (PPHT) on Al composites manufactured by FSP wherein SiC [19], TiB_2 [20], and Al_2O_3 [21] were used as reinforcing particulates. Yet, little is known about the effect of post-processing heat treatment on AA2024/Al_2O_{3p} composites produced by FSP. Up to our

✉ Adel Haddad
adel.haddad@hotmail.com

[1] Laboratoire d'Etudes et Recherche en Technologie Industrielle, LERTI, University of Saad Dahleb Blida 1, Blida, Algeria

[2] Laboratory of Structures, University of Saad Dahleb Blida 1, Blida, Algeria

[3] Research Center in Industrial Technologies CRTI, P.O. Box 64, Cheraga, Algiers, Algeria

[4] Laboratoire des Sciences et Génie des Matériaux, USTHB, Algiers, Algeria

Table 1 Chemical composition of as-received aluminum alloy 2024-T351

Al	Cu	Mg	Mn	Si	Fe	Zn	Ti
Balance	4.6	1.3	0.65	0.43	0.5	0.25	0.15

knowledge, only El-Mahallawi et al. [10] worked on PPHT of this composite system, and they reported improvement in ultimate tensile strength, elongation, and hardness after solution treatment followed by T6 aging treatment on 2024 alloy prepared by semisolid casting. In pursuit of what has been done, the main impetus of this work is devoted to understanding the post-processing heat treatment (PPHT) effect on microstructure, hardness, wear behavior, and precipitation mode of AA2024/Al_2O_3 FSPed surface composite.

2 Materials and methods

The chemical composition of the Al alloy 2024-T351 sheets used in this study is listed in Table 1. The chemical analysis of the metal sheets was tested using stationary optical emission spectrometer (Oxford, Foundry Master Pro). Before friction stir processing, the sheets were cleaned with acetone and alcohol. The groove with a squared shape of 2.5mm width and 3mm depth was filled with alumina powder (size: 1μm, provider: Sigma Aldrich). A pinless tool was used to seal the groove with the same FSP parameters; then, the sheets were submitted to one and three passes of the tool (pin: circular profile, 6mm diameter, and 3mm length; shoulder: circular profile, 20 mm diameter), at 1400 rpm rotational speed and 40mm transverse speed. The schematic of the working mechanism of setting FSP parameters is shown in Fig. 1. The

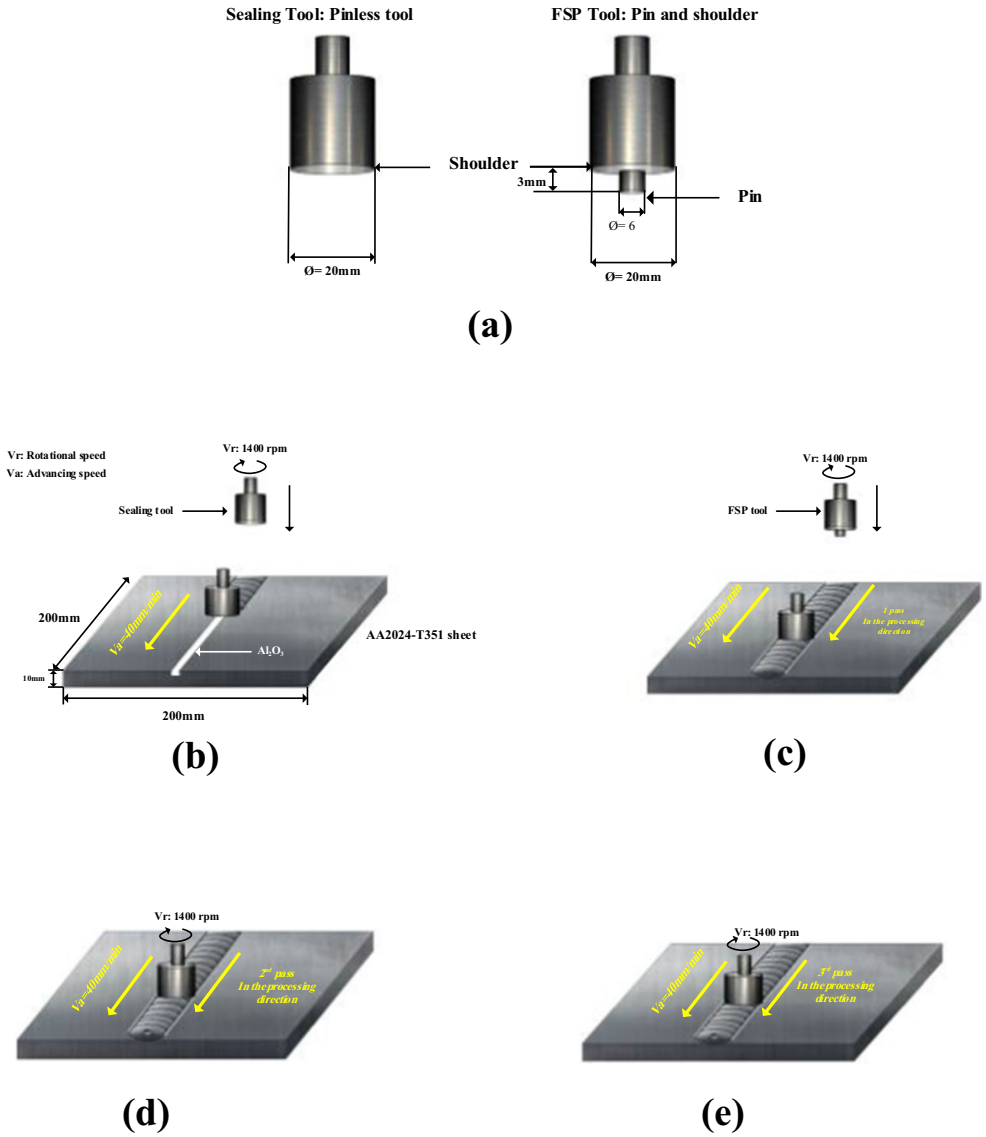

Fig. 1 Schematic of the working mechanism of friction stir process: **a** pinless and FSP tool dimensions, **b** working process of Al_2O_3 powder insertion and sealing the groove, and **c**–**e** schematic of the 1st, 2nd, and 3rd pass of FSP, respectively

FSPed composites were heat-treated in an open-air furnace (Nabertherm GmbH, Germany) consisting of solutionizing at 530°C, subsequent quenching in water, followed by aging treatment at 180°C for 8 h.

The X-ray diffraction (XRD) analysis was done with a Brucker Advance 8 diffractometer with copper radiation. The FSPed samples were cross-sectioned and mechanically grounded with SiC abrasive paper and finished with a diamond solution before the metallographic examination. The Scanning Electron Microscope, SEM (Quanta 650; FEI Netherlands), equipped with an Energy Dispersive X-ray spectrometer, EDS, (Bruker X-Flash 6/10) was used to study the microstructure and the worn tracks of the AA2024-T351/Al_2O_{3p} composites.

Vickers microhardness measurements were performed for each sample by applying 100 gf load for a 10s holding time, using a commercial micro-indenter (CSM Instruments, Switzerland) Berkovich diamond tip. The microhardness profiles were done at 1mm and 2mm depth from the sample FSPed surface, and more than three measurements were taken.

Wear tests were done at the top surface of the FSP zone, using a rotary ball-on-disc tribometer (CSM instrument, Switzerland) under 4N load at 15 cm/s sliding speed, for a total distance of 300m. The wear experiments were done at room temperature, under dry sliding by pressing a 6-mm 100Cr6 steel ball, at 40% relative humidity. The load and sliding speed parameters were chosen based on the work by Zhang and Alpas on the wear maps and wear regime transition in AA6061 [22] and in AA6061-reinforced Al_2O_3 composites [23], sliding against 100Cr6 steel. The present applied load (4N load) falls in the wear regime I (see ref. [23]) for reinforced Al_2O_3/Al composite and in wear regime II for unreinforced Al alloy, wherein the reinforcement effect (Al_2O_{3p}) is relevant [23].

3 Results

3.1 Microstructure of FSPed AA2024/Al_2O_{3p} surface composites

Figure 2a shows the XRD pattern of the as-received AA2024-T351 used in this study. The pattern indicates the presence of only Al peaks. The Al alloy 2024 is an age hardenable alloy through the precipitation of Al_2Cu and Al_2CuMg phases [18]. Herein, these precipitations could not be detected through our XRD analysis. Image analysis by SEM of the AA2024-T351 surface has shown the presence of coarsening Al_2Cu or Al_2CuMg phases (white particles) identified by EDS (Table 2), where the darker contrast is Al matrix (Fig.

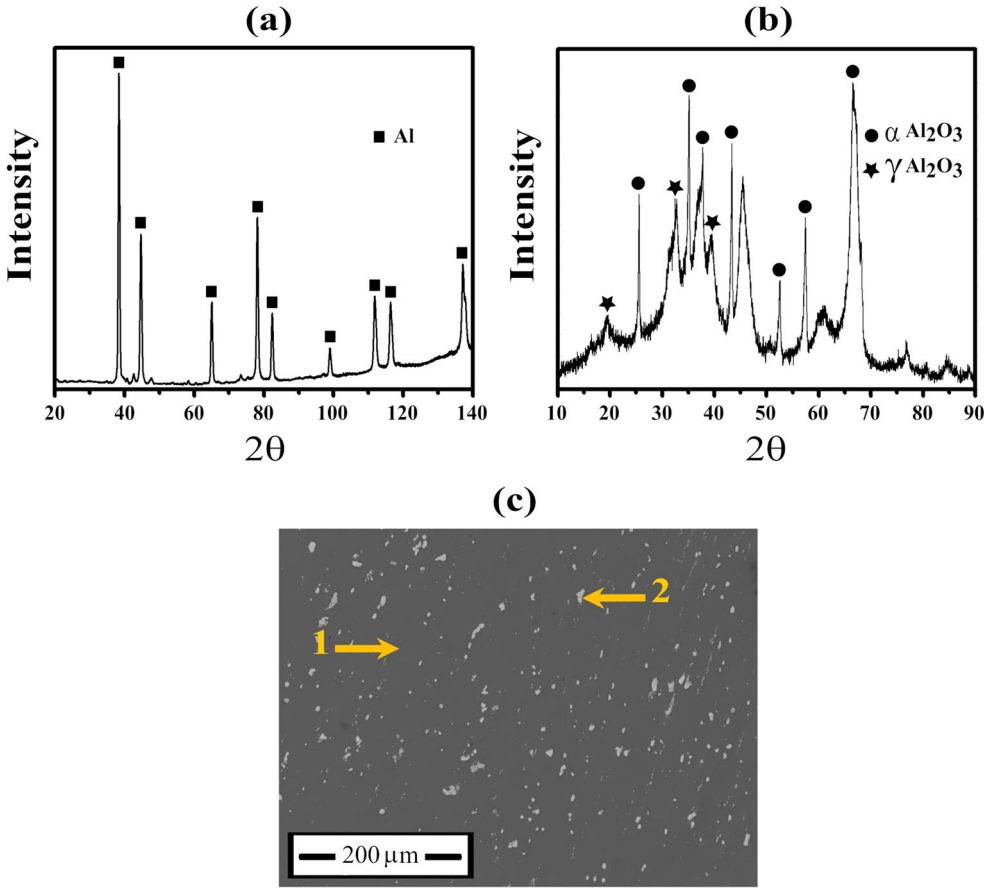

Fig. 2 X-ray diffraction patterns of **a** AA2024-T351 and **b** alumina powder. **c** SEM-EDS of as-received AA2024-T351

2c). The XRD pattern of Al_2O_3 powders (Fig. 2b) shows major peaks of two predominantly alumina phases: α Al_2O_3 and γ Al_2O_3.

SEM microstructure of the AA2024-T351/Al_2O_{3p} surface composite is shown in Fig. 3a, after three cycles of the friction stir processing. A defect-free stir zone was partially achieved with nearly homogenous distribution of the Al_2O_{3p} particles inside the Al alloy matrix. The reinforcement particle size decreased from micron to submicron size due to powder fragmentation during FSP [13–15, 19, 20]. The SEM-EDS elemental mapping is shown in Fig. 3b–e. Oxygen distribution through the Al matrix revealed acceptable dispersion of Al_2O_3 particles. Multi-pass (three passes) FSP exhibited a microstructure clear from voids and tunnel defect.

Figure 4 shows microhardness profiles of the three-pass FSPed AA2024-T351/Al_2O_{3p} before and after post-processing heat treatment, which was carried out on a cross-section of the samples. Microhardness values decreased in the heat-affected zone (HAZ) and nugget zone after subsequent FSP (Fig. 4a); this was due to the dissolution of hardening precipitates Al_2Cu [21]. The integration of Al_2O_{3p} increased the hardness of the processed surface composites to a mean microhardness value of 150HV, as shown in Fig. 4b.

Further tailoring of hardness property could be done by heat treatments after FSP to homogenize the microstructure. In 2024-T351 alloys, heat treatments were extensively studied in many previous scientific reports [24, 25]. The heat treatment was chosen based on the work of Zhang and Alpas [26] on 2024 alloys, consisting of solutionizing at 530°C, subsequent quenching, followed by aging treatment at 180°C for 8 h. The microhardness profiles indicated a slight increment in microhardness average values; the microhardness of heat-affected zone was successfully recovered (Fig. 4c). However, many low values were recorded in the stirred zones (SZs).

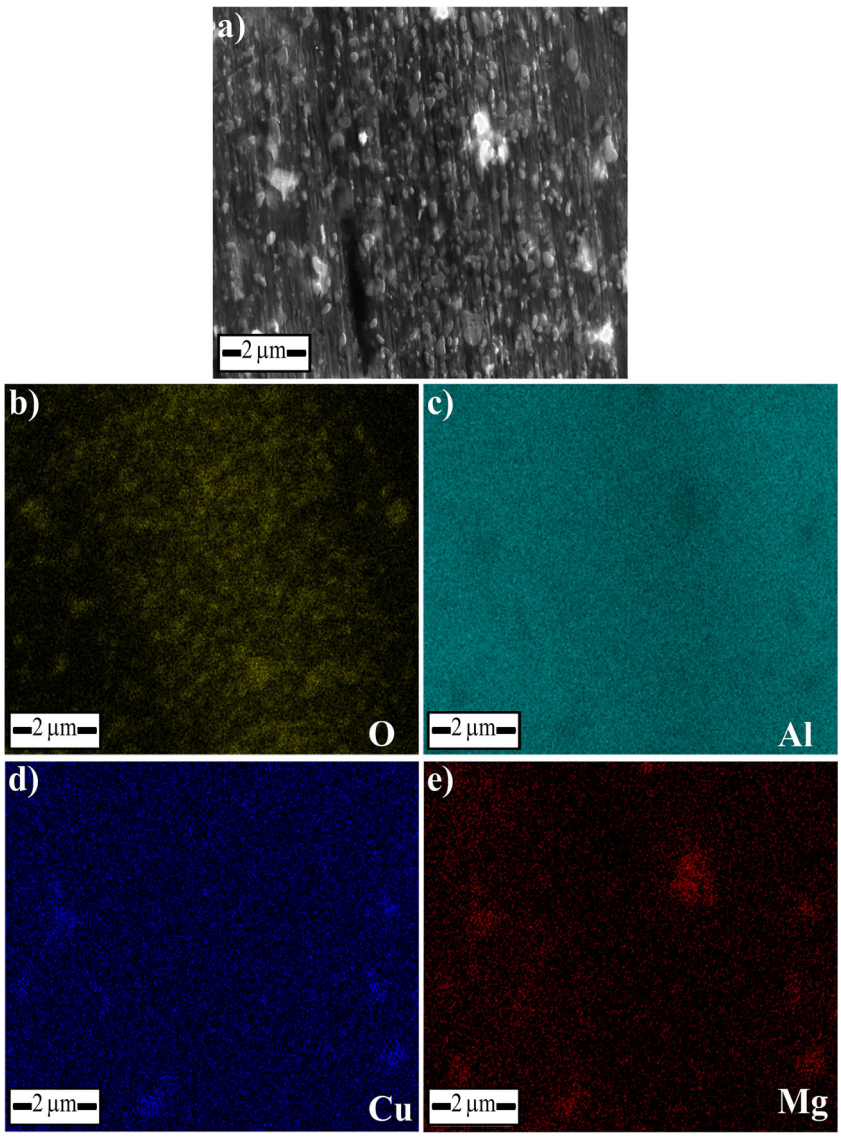

Fig. 3 **a** SEM of the AA2024-T351/Al_2O_{3p} stir zone composite and SEM-EDS elemental mapping of **b** oxygen, **c** aluminum, **d** copper, and **e** magnesium

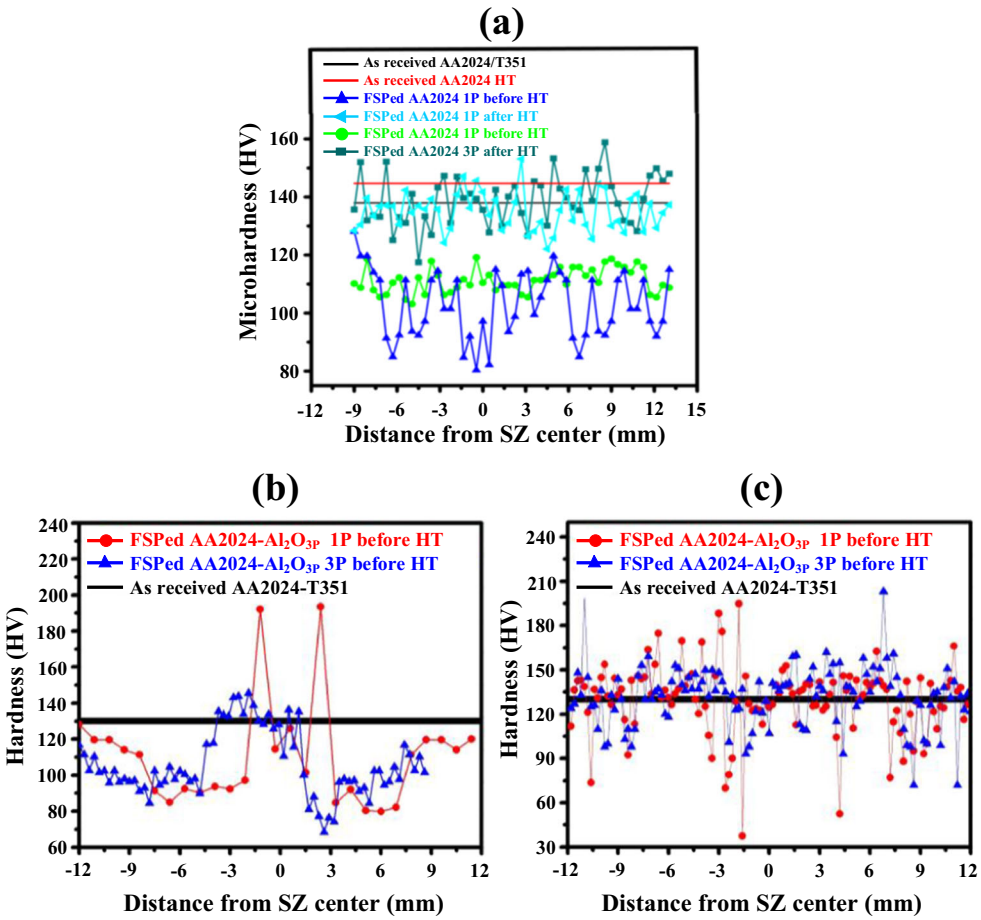

Fig. 4 Microhardness profiles of as-received, as friction stir processed areas after and before heat treatment without Al_2O_{3p} incorporation (**a**), AA2024-T351/Al_2O_{3p} surface composites before (**a**) and after heat treatment (**c**)

After heat treatment, different microstructural features were observed, as shown in Fig. 5. The Al_2O_3 particles as well as precipitates were agglomerated inside grain boundaries of the Al alloys matrix. Figure 5a shows the interface between the FSPed zone and unprocessed zone, after heat treatment. Higher magnification of the heat-treated FSPed zone (Fig. 5b) shows different microstructural features compared to as-FSPed surface composite (Fig. 3). EDS analysis in this region showed intermixed elements from both Al_2O_{3p} particles and AA2024 elements (spots: 3–5, Table 3). The most intriguing phenomenon found herein is in the heat-affected zone (HAZ); it was affected by the PPHT in a way that has never been reported previously. The precipitation mode changed to what is a grain boundary precipitation (Fig. 5c). EDS spots (6–8, Table 3) marked in Fig. 5d show that these precipitations consist of a coarsen Al_2Cu and some intermetallic phase mixture.

A top view of the surface composite 2024/Al_2O_{3p} FSPed at the SZ, after heat treatment, is shown in Fig. 6. Compared to the HAZ (Fig. 5c), the grain size has been reduced due to the stirring action of the FSP tool. Moreover, both these regions underwent precipitation at grain boundaries. It must be noted that swelling behavior was obvious by naked eye at the surface of the FSPed composite as well as extensive pore creation in the SZ.

Further investigation of the heat-treated surface composite in the FSPed zone was done by EDS elemental mapping (Fig. 7). Oxygen, copper, and magnesium distribution revealed that Al_2O_3 particles were attracted to agglomerate at grain boundaries along with Cu and Mg (Fig. 7b–e), causing their depletion in the Al matrix.

Table 2 Summary of EDS spots, in at.%, of as-received AA2024-T351 (Fig. 1c). Numbers in first column correspond to point's number indicated in the figure. The nominal compositions are listed in last column

Location	Al	Cu	Mg	Nominal comp.
1	97.4	1.3	1.3	$Al_{97}Cu_1Mg_2$
2	58.4	21.5	20.1	$Al_{58}Cu_{22}Mg_{20}$

3.2 Friction and wear behavior of AA2024/Al_2O_3p surface composites

Figure 8 shows the friction coefficient (μ) variation with sliding distance and corresponding wear scar 2D profiles. For unprocessed AA2024 before and after heat treatment, the μ starts at high values and decreases to lower steady-state

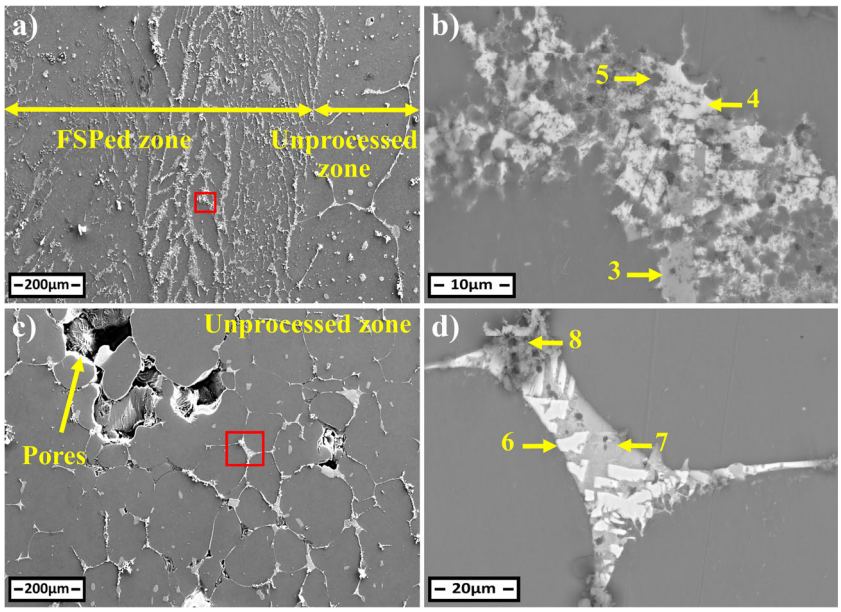

Fig. 5 SEM-EDS of heat-treated AA2024/Al_2O_{3p} composites. **a** Interface between the friction stir processed zone and unprocessed zone. **b** Higher magnification of red square in **a**. **c** Heat-affected zone (unprocessed zone) and **d** higher magnification of red square in **c**

values. On the other hand, for AA2024/Al_2O_{3p} surface composites, the μ decreases with increasing the FSP cycles, and lower μ values were recorded for untreated samples. In means of wear resistance, the material removal rate of the FSPed AA2024/Al_2O_{3p} surface composites before heat treatment was lower compared to as-received alloy. However, after heat treatment, the wear resistance of the composites decreased to the same removal rate of the unprocessed 2024 alloy. The highest wear resistance was attributed to the FSPed surface composites after 3 cycles, without heat treatment.

Worn track SEM micrographs of unreinforced surface composites (Fig. 9) showed signs of delamination (spalling), pits, and cracks relatively perpendicular to the sliding direction; the latters are signs of adhesive wear, while the grooves parallel to the sliding direction are showing evidence of an abrasive wear mechanism. Plowing wear was highly seen on the unreinforced alloy compared to Al_2O_{3p}-reinforced AA2024 surface composites, as shown in Fig. 10. The dominant wear mechanisms in the case of surface composites were less adhesive and more abrasive compared to unreinforced Al 2024 alloy. Comparative EDS analyses on the tribolayers formed on both unreinforced and reinforced AA2024 matrix are both showing the presence of Al, O, and traces of Mn, Cu, and Mg. However, for reinforced composites before and after heat treatment, a small presence of Fe was perceivable in the tribolayer composition.

4 Discussion

Many microstructural studies on different FSP zones were extensively reported in the literature. The heat generation during the friction between the FSP tool and workpiece causes dissolution and partial re-precipitation inside the nugget zone (NZ), grain deformation in the thermo-mechanically affected zone (TMAZ), and precipitation coarsening in the heat-affected zone (HAZ) [14–17, 20, 21]. As the metal matrix is deformed at a high temperature and individual grains experience diverse stages of straining, this highly transient microstructure type demonstrates different mechanical properties.

Microhardness of AA2024-T351 was enhanced by integrating the Al_2O_{3p} compared to FSPed sample. This behavior

Table 3 Summary of EDS spots, in at.%, of FSPed composites (Fig. 4). Numbers in first column correspond to point's number indicated in the figure. The nominal composition is listed in last column

Location	Al	Cu	Mg	O	Si	Fe	Mn	Nominal comp.
3	83.07	2.59	0.34	–	–	7.7	6.29	$Al_{83}Cu_3Mg_1Fe_8Mn_6$
4	67.8	10.3	7.8	11	1.6	0.7	0.7	$Al_{68}Cu_{10}Mg_8O_{11}Si_2Fe_1Mn_1$
5	53.2	18.5	11	14.4	1.6	1	0.5	$Al_{53}Cu_{18}Mg_{11}O_{14}Si_2Fe_1Mn_1$
6	63.4	24.4	6	4.9	1.4	–	–	$Al_{63}Cu_{24}Mg_6O_5Si_1$
7	51.2	15	12.4	19.7	1.7	–	–	$Al_{51}Cu_{15}Mg_{12}O_{20}Si_2$
8	38	11.6	6.4	44	–	–	–	$Al_{38}Cu_{12}Mg_6O_{44}$

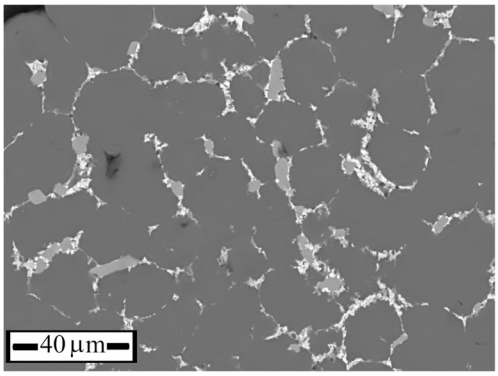

Fig. 6 Stir zone top view of the heat-treated AA2024 /Al_2O_{3p} composite's microstructure

has been well reported for AMCs reinforced by Al_2O_{3p} [11, 16, 27]; besides grain refining due to severe plastic deformation induced by FSP, the alumina particles contribute to further refinement of the microstructure's grain size during the recrystallization process in the nugget zone. Another factor and most importantly, alumina particles restrict the dislocations' movement through the Orowan mechanism effect. Hence, in Al/Al_2O_{3p} FSPed surface composites both ex situ incorporated particles and Al_2Cu precipitates contribute to Orowan strengthening and the strengthening through Hall-Petch effect induced by FSP. The aforementioned effects enhanced the hardness of the Al/Al_2O_{3p} surface composites.

In previous works, many researchers reported the effect of heat treating Al-Si alloys reinforced with Al_2O_{3p} [9].

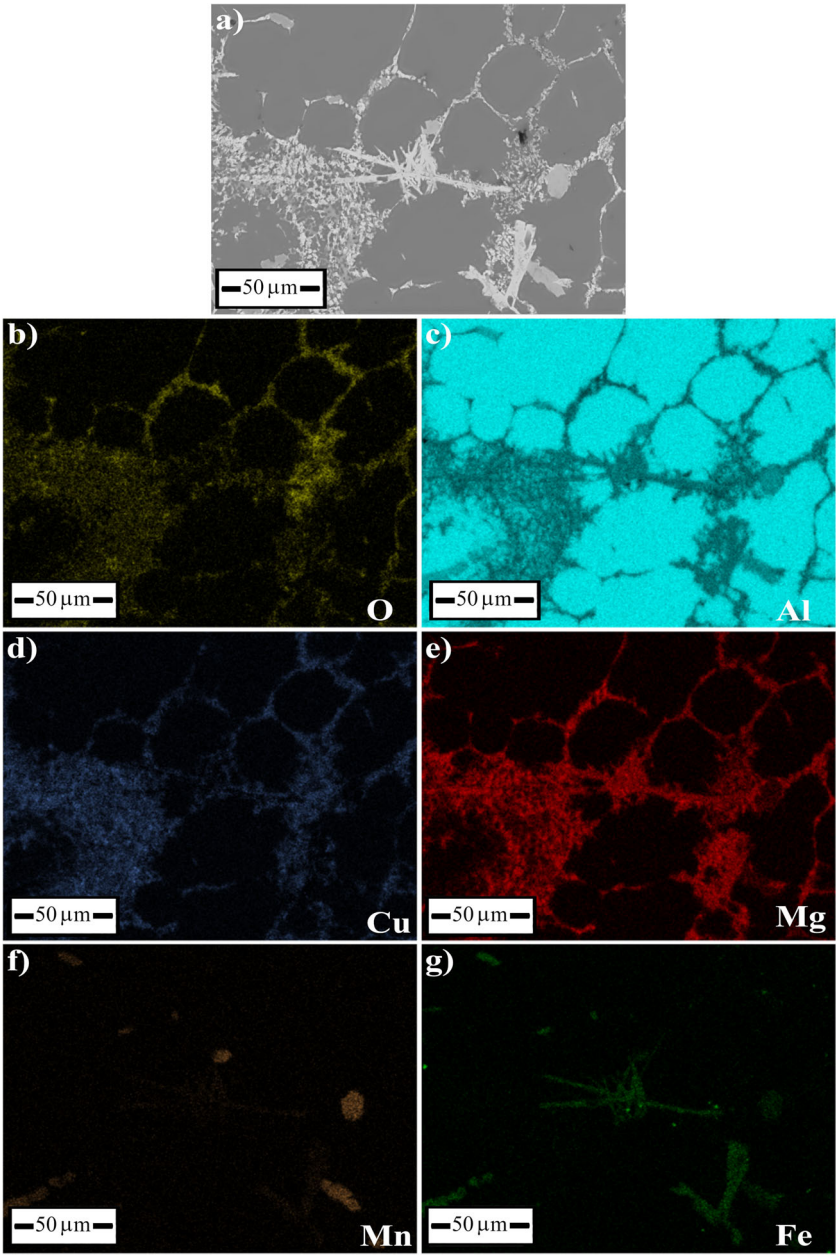

Fig. 7 SEM-EDS elemental mapping of heat-treated AA2024-T351/Al_2O_{3p} surface composite

However, few research works have been devoted to Mg containing Al alloys reinforced with Al_2O_{3p}. It has been reported that the formation of Al_2MgO_4 spinel deteriorated the mechanical properties of the composites [8, 9] when others reported on its beneficial effect [16]. Tekmen and Cocen [28] solved this issue, and they stated that Al_2MgO_4 affects positively the AMC if the spinel is formed homogeneously at the particle/matrix interface, where it does the contrary if its formation is discontinuous. Al_2MgO_4 spinel forms in 2024 alloys because of the higher Mg to Si content [29], and the Si content could be increased in Al/Al_2O_3 composites to form Mg_2Si precipitates rather than the spinel phases.

The elemental distribution shown in Fig. 7 presents probably the formation of spinel phases such as Al_2MgO_4 or Al_2CuO_4 through the reaction of Al_2O_3 and matrix elements. Herein, it is assumed that the complete disappearing of Al_2O_3 particles is more probable, where the total formation of the spinel phase is expected; future investigations are needed to confirm the above statements.

At 530°C, some liquid Al forms at the grain boundaries [18] and facilitates the O diffusion released during the reaction of Al_2O_3 and Mg during the formation of the spinel phases [30, 31]. This grain boundary precipitation causes a slight increment of the hardness values after heat treatment. On the other hand, the voids and pores were responsible for hardness drop, explaining such low values in microhardness profiles. It was previously reported that alumina particle incorporation accelerates the precipitation mechanism in precipitation-hardened Al-Si alloys [32]. Based on the totality of these results, it is reasonable to conclude that heat treatment of 530°C for 2h causes an over-aging behavior of AA2024/Al_2O_{3p} surface composites, which affects the precipitation mechanisms, in both SZ and HAZ. Any greater attractive forces of the Cu or Mg, such their attraction to Al_2O_3 particles, should be taken into account or the hardening mechanisms would not be activated. To avoid such issues, it is likely to design 2024 with higher Si/Mg content because of the high affinity of Mg with Si to form Mg_2Si compared to Mg with Al_2O_{3p}.

Grain boundary precipitation is known to decrease the fracture toughness and formability of aluminum alloys, which could be the reason for deterioration of wear resistance of heat-treated AA2024/Al_2O_3 [33, 34]. Steele et al. [35] studied the influence of quenching rate on the grain boundary precipitation extent on 6XXX aluminum alloys after solution heat treatment, and it was shown that as the quenching rate decreased, the grain boundary precipitation increased. It is known that Al_2O_3 particles decrease the thermal conductivity of Al matrix; thus, it may affect the quenching rate of the studied composite [36]. In metals including Al alloys, the conductivity is generally correlated with strength and hardness of the material. A higher strength is usually accompanied with a lower electrical conductivity and vice versa [37]. After PPHT, the hardness values increased; thus, it is expected that the material conductivity decreases [38]. It should be noted that many factors could influence the conductivity such as type and nature of precipitates, grain boundary precipitation, grain size, dislocation density, and crystalline defects [37, 38]. Hence, it could not firmly be confirmed that material conductivity decreased only by strength correlation, without taking all these factors in consideration.

The second reason could be caused by the thermal history induced by FSP. As FSP causes coarsening of precipitates, hardness was frequently seen to decrease in the HAZ due to grain boundary precipitation [39]. The driving force for precipitation is caused by heat and nucleation sites; Liu et al. [40] showed that HAZ presents low dislocation density due to different microstructural changes in 7075AA matrix under

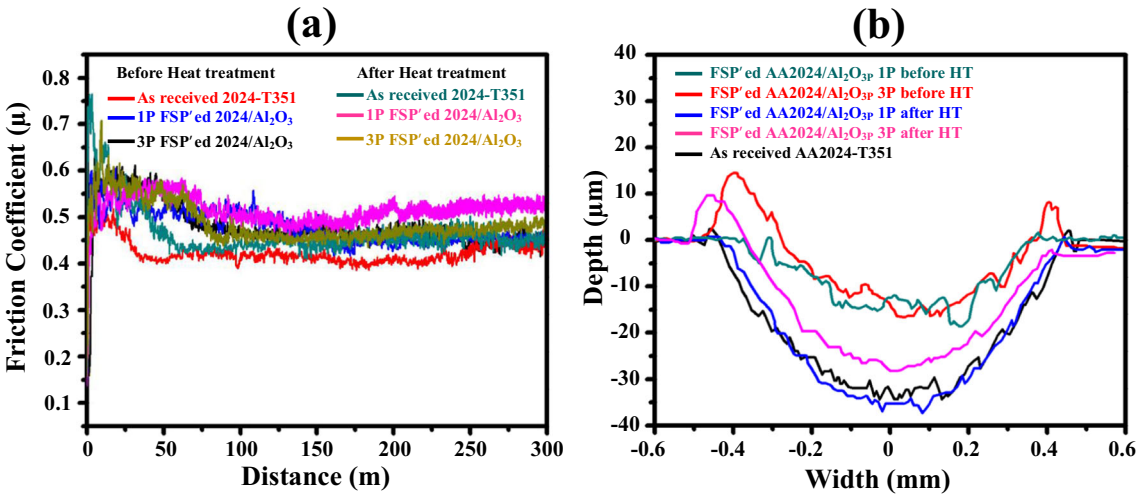

Fig. 8 **a** Evolution of friction coefficient versus sliding distance before and after heat treatment for unreinforced AA2024 and reinforced alumina surface composites. **b** 2D profiles of as-received AA2024-T351 and reinforced Al_2O_{3p}

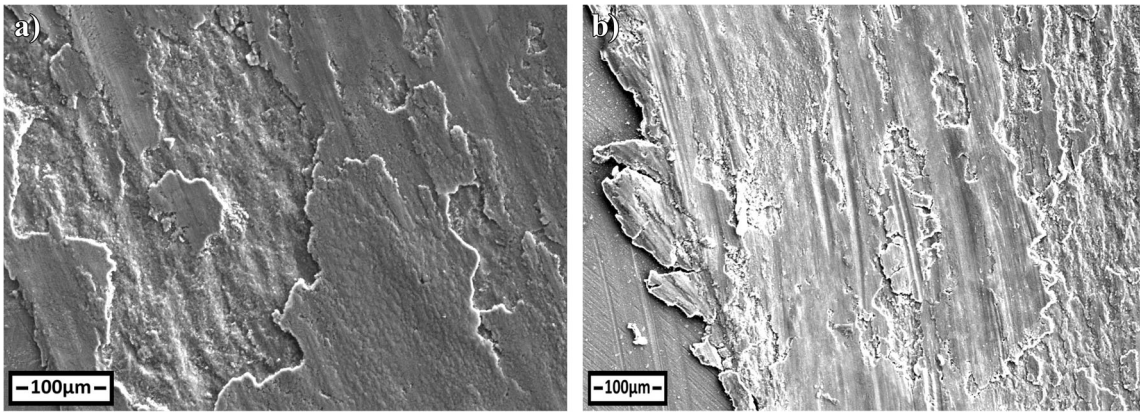

Fig. 9 Worn surfaces of **a** as-received AA2024-T351 and **b** heat-treated AA2024 without Al_2O_{3p} reinforcements

the FSW thermal cycle. Reducing the number of dislocations will reduce the nucleation sites at grain interior; hence, grain boundary precipitation is more probable to occur.

Thirdly, oxygen migration from SZ to HAZ could be responsible for grain boundary precipitation as occurred in HAZ; as evidence of EDS point 8, some areas showed oxygen presence. However, EDS should be taken by a grain of salt in quantifying oxygen. Therefore, more works are needed to understand the main factor responsible for this phenomenon in the present FSPed composite system.

The wear scars of AA2024/Al_2O_{3P} surface composites before and after heat treatment were characterized by a transition from adhesive to a more dominant abrasive wear mechanism, as shown in Fig. 10. The abrasive wear is due to de-cohesion and de-bonding of the hard Al_2O_3 particles as third-body abrasive particles. The less adhesive action is due to the hardening of the Al matrix; alumina enhanced the load bearing of the sliding steel ball and minimized the wearing by adhesive wear. It was previously reported [23, 41] that the delamination through adhesive wear is triggered by the crack initiation and growth at the subsurface mechanically mixed layers formed on the wear scars. Heat generation during dry sliding wear decreased the plasticity of the aluminum alloys, which decreases the toughness and ultimate mechanical resistance of the matrix. Thus, it causes a premature failure of this subsurface layer. Another possible effect of the surface composite wear resistance compared to unreinforced alloy is due to the low conductivity of the Al_2O_{3p} particles which prevented the heat dissipation during sliding wear, hence delayed the delamination of the mechanically mixed layers (MMLs), resulting in less adhesive wear mechanism.

Contrary to the unreinforced alloy, the EDS analysis revealed the presence of Fe in the tribolayers (or MML) formed on the composite worn surfaces. The iron were transferred from the sliding ball to the composite surface and further oxidized due to the abrasive actions of Al_2O_{3p}. It has been reported extensively the beneficial effect of Fe-containing tribolayers on the wear and friction behavior of many metal

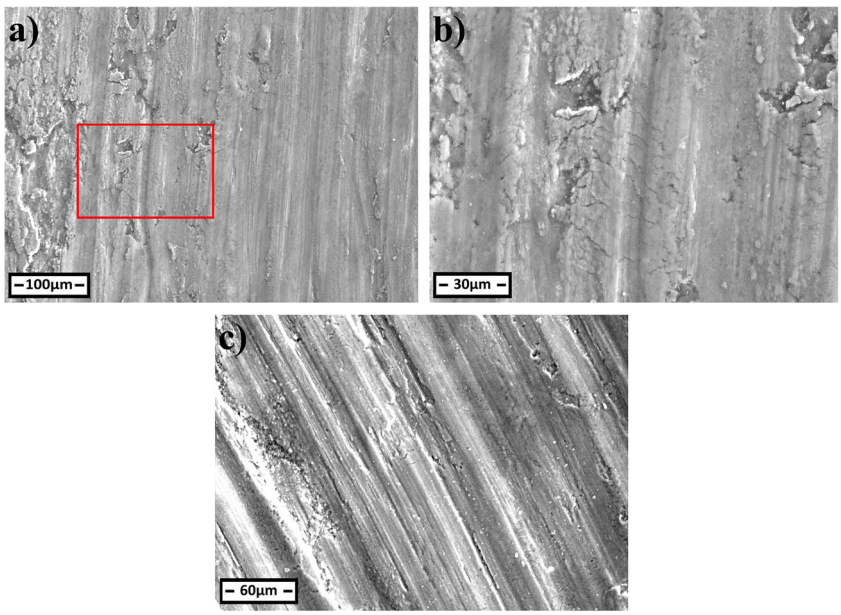

Fig. 10 Worn surfaces of **a** as-FSPed AA2024-T351/Al_2O_{3p}, **b** higher magnification of red square marked in **a**, and **c** heat-treated AA2024/Al_2O_{3p} composites

matrix composites [23, 41, 42]. Fe-containing tribolayers could also be the cause of the wear resistance enhancement.

The heat treatment did not change the wear mechanisms for AA2024/Al_2O_{3p} composites, and the low wear resistance of heat-treated AA2024/Al_2O_{3P} composite is due probably to the pores and voids that triggered high wear and material removal. Hence, it can be concluded that over-aging heat treatment on AA2024/Al_2O_{3p} composites has a detrimental effect on the wear resistance.

5 Conclusion

Herein, AA2024 surface composites were processed by inserting Al_2O_{3p} particles as reinforcements through the friction stir processing route. The effect of heat treatment on microstructure and wear behavior was studied; the main conclusions are as follows:

Integrating Al_2O_{3P} particles inside the AA2024 matrix enhanced its hardness to an average value of 150 HV as well as wear resistance by a factor of two.

Heat treating the surface composite did not have any beneficial effect on wear resistance or hardness, except recovering the HAZ's hardness.

After heat treatment, Al_2O_{3P} particles reacted with Cu and Mg to form spinel phases and precipitated at the grain boundaries. Moreover, the precipitation mode in the HAZ changed to a precipitation at grain boundaries; this was caused probably by the thermal history induced by FSP.

Acknowledgements The authors would like thank Air Algérie company for providing the Al alloy 2024-T351 sheets. Special thanks to Miss Selma Hanifi and Mr. Walid Bedjaoui of Research Center in Industrial Technologies (CRTI) for their help during SEM and XRD characterization. This work was supported by Direction Générale de la Recherche Scientifique et du Développement Technologique (DGRSDT), Algeria.

Author contribution Adel Haddad and Abdessabour Benamor were responsible for the experimental work, Nabil Chiker and Youcef Hadji carried out the XRD analysis, Maamar Hakem and Riad Badji were responsible of the SEM analysis, Said Abdi assured tribological testing, and Mustapha Temmar and Mohamed Hadji contributed to making the final draft of the paper. All the authors read and approved the final manuscript.

Funding This work was supported by the Algerian general directory of scientific research and technological development (DGRSDT), Algeria.

Availability of data and material Not applicable.

Code availability Not applicable.

Declarations

Conflict of interest The authors declare no competing interests.

References

1. Kok M (2005) Production and mechanical properties of Al2O3 particle-reinforced 2024 aluminium alloy composites. J Mater Process Technol 161:381–387. https://doi.org/10.1016/j.jmatprotec.2004.07.068
2. Kök M, Özdin K (2007) Wear resistance of aluminium alloy and its composites reinforced by Al2O3 particles. J Mater Process Technol 183:301–309. https://doi.org/10.1016/j.jmatprotec.2006.10.021
3. Ünlü BS (2008) Investigation of tribological and mechanical properties Al2O3–SiC reinforced Al composites manufactured by casting or P/M method. Mater Des 29:2002–2008. https://doi.org/10.1016/j.matdes.2008.04.014
4. Abdel-Azim AN, Shash Y, Mostafa SF, Younan A (1995) Casting of 2024-Al alloy reinforced with Al2O3 particles. J Mater Process Technol 55:199–205. https://doi.org/10.1016/0924-0136(95)01954-5
5. Sajjadi SA, Ezatpour HR, Beygi H (2011) Microstructure and mechanical properties of Al-Al2O3 micro and nano composites fabricated by stir casting. Mater Sci Eng A 528:8765–8771. https://doi.org/10.1016/j.msea.2011.08.052
6. Xu H, Zhang G, Cui W, Ren SB, Wang QJ, Qu XH (2018) Effect of Al2O3sf addition on the friction and wear properties of (SiCp+Al2O3sf)/Al2024 composites fabricated by pressure infiltration. Int J Miner Metall Mater 25:375–382. https://doi.org/10.1007/s12613-018-1581-z
7. Daoud A, Abou El-Khair MT, Abdel-Azim AN (2004) Effect of Al2O3 particles on the microstructure and sliding wear of 7075 Al alloy manufactured by squeeze casting method. J Mater Eng Perform 13:135–143. https://doi.org/10.1361/10599490418325
8. Lloyd DJ (1994) Particle reinforced aluminium and magnesium matrix composites. Int Mater Rev 39:1–23. https://doi.org/10.1179/imr.1994.39.1.1
9. Forn A, Teresa Baile M, Rupérez E (2003) Spinel effect on the mechanical properties of metal matrix composite AA6061/(Al2O3)p. J Mater Process Technol 143–144:58–61. https://doi.org/10.1016/S0924-0136(03)00319-4
10. El-Mahallawi I, Ahmed MMZ, Mahdy AA et al (2017) Effect of heat treatment on friction-stir-processed nanodispersed AA7075 and 2024 Al alloys BT - friction stir welding and processing IX. In: Hovanski Y, Mishra R, Sato Y et al (eds) . Springer International Publishing, Cham, pp 297–309
11. Schultz BF, Ferguson JB, Rohatgi PK (2011) Microstructure and hardness of Al2O3 nanoparticle reinforced Al-Mg composites fabricated by reactive wetting and stir mixing. Mater Sci Eng A 530:87–97. https://doi.org/10.1016/j.msea.2011.09.042
12. Wang N, Wang Z, Weatherly GC (1992) Formation of magnesium aluminate (spinel) in cast SiC particulate-reinforced Al(A356) metal matrix composites. Metall Trans A 23:1423–1430. https://doi.org/10.1007/BF02647325
13. Vani VV, Chak SK (2018) The effect of process parameters in aluminum metal matrix composites with powder metallurgy. Manuf Rev 5. https://doi.org/10.1051/mfreview/2018001
14. Sharma V, Prakash U, Kumar BVM (2015) Surface composites by friction stir processing: a review. J Mater Process Technol 224:117–134. https://doi.org/10.1016/j.jmatprotec.2015.04.019
15. Rathee S, Maheshwari S, Siddiquee AN (2018) Issues and strategies in composite fabrication via friction stir processing: a review. Mater Manuf Process 33:239–261. https://doi.org/10.1080/10426914.2017.1303162
16. Hoziefa W, Toschi S, Ahmed MMZ, Morri A, Mahdy AA, el-Sayed Seleman MM, el-Mahallawi I, Ceschini L, Atlam A (2016) Influence of friction stir processing on the microstructure and mechanical properties of a compocast AA2024-Al2O3 nanocomposite. Mater Des 106:273–284. https://doi.org/10.1016/j.matdes.2016.05.114

17. Moustafa E (2017) Effect of multi-pass friction stir processing on mechanical properties for AA2024/Al2O3 nanocomposites. Materials 2017, 10, 1053. https://doi.org/10.3390/ma10091053
18. Bharti S, Ghetiya ND, Patel KM (2020) Micro-hardness and wear behavior of AA2014/Al2O3 surface composite produced by friction stir processing. SN Appl Sci 2:1760. https://doi.org/10.1007/s42452-020-03585-2
19. Ghanbari D, Kasiri Asgarani M, Amini K, Gharavi F (2017) Influence of heat treatment on mechanical properties and microstructure of the Al2024/SiC composite produced by multi–pass friction stir processing. Measurement 104:151–158. https://doi.org/10.1016/j.measurement.2017.03.024
20. Geng J, Hong T, Ma Y, Wang M, Chen D, Ma N, Wang H (2016) The solution treatment of in-situ sub-micron TiB2/2024 Al composite. Mater Des 98:186–193. https://doi.org/10.1016/j.matdes.2016.03.024
21. Refat M, Abdelmotagaly AMM, Ahmed MMZ, El-Mahallawi I (2016) The effect of heat treatment on the properties of friction stir processed AA7075-O with and without nano alumina additions BT - friction stir welding and processing VIII. In: Mishra RS, Mahoney MW, Sato Y, Hovanski Y (eds) . Springer International Publishing, Cham, pp 115–123
22. Zhang J, Alpas AT (1997) Transition between mild and severe wear in aluminium alloys. Acta Mater 45:513–528. https://doi.org/10.1016/S1359-6454(96)00191-7
23. Zhang J, Alpas AT (1993) Wear regimes and transitions in Al2O3 particulate-reinforced aluminum alloys. Mater Sci Eng A 161:273–284. https://doi.org/10.1016/0921-5093(93)90522-G
24. Hannard F, Castin S, Maire E, Mokso R, Pardoen T, Simar A (2017) Ductilization of aluminium alloy 6056 by friction stir processing. Acta Mater 130:121–136. https://doi.org/10.1016/j.actamat.2017.01.047
25. Ghanbari D, Asgarani MK, Amini K, Gharavi F (2017) Influence of heat treatment on mechanical properties and microstructure of. Measurement. 104:151–158. https://doi.org/10.1016/j.measurement.2017.03.024
26. Jang J-H, Nam D-G, Park Y-H, Park I-M (2013) Effect of solution treatment and artificial aging on microstructure and mechanical properties of Al–Cu alloy. Trans Nonferrous Metals Soc China 23:631–635. https://doi.org/10.1016/S1003-6326(13)62509-1
27. Yang K, Li W, Niu P, Yang X, Xu Y (2018) Cold sprayed AA2024/Al2O3 metal matrix composites improved by friction stir processing: microstructure characterization, mechanical performance and strengthening mechanisms. J Alloys Compd 736:115–123. https://doi.org/10.1016/j.jallcom.2017.11.132
28. Tekmen C, Cocen U (2003) The effect of Si and Mg on age hardening behavior of Al-SiCp composites. J Compos Mater 37:1791–1800. https://doi.org/10.1177/002199803035181
29. Mitchell CA, Davidson AM (2000) Effect of Al2O3 particulates as reinforcement in age hardenable aluminium alloy composites. Mater Sci Technol 16:873–876. https://doi.org/10.1179/026708300101508595
30. Cöcen Ü, Önel K, Özdemir I (1997) Microstructures and age hardenability of AL-5%si-0.2%Mg based composites reinforced with particulate SiC. Compos Sci Technol 57:801–808. https://doi.org/10.1016/S0266-3538(97)00049-3
31. Li W, Liao NM, Jiang YD, Shen BL (2007) Interface study of short mullite fibre reinforced Al–Cu–Mg alloy composites. Mater Sci Technol 23:229–232. https://doi.org/10.1179/174328407X157254
32. Das T, Munroe PR, Bandyopadhyay S (1996) The effect of Al2O3 particulates on the precipitation behaviour of 6061 aluminium-matrix composites. J Mater Sci 31:5351–5361. https://doi.org/10.1007/BF01159304
33. Briant CL (2001) Grain boundary structure, chemistry, and failure. Mater Sci Technol 17:1317–1323. https://doi.org/10.1179/026708301101509331
34. Li BQ, Reynolds AP (1998) Correlation of grain-boundary precipitates parameters with fracture toughness in an Al–Cu–Mg–Ag alloy subjected to long-term thermal exposure. J Mater Sci 33:5849–5853. https://doi.org/10.1023/A:1004426820624
35. Steele D, Evans D, Nolan P, Lloyd DJ (2007) Quantification of grain boundary precipitation and the influence of quench rate in 6XXX aluminum alloys. Mater Charact 58:40–45. https://doi.org/10.1016/j.matchar.2006.03.007
36. Tatar C, Özdemir N (2010) Investigation of thermal conductivity and microstructure of the α-Al2O3 particulate reinforced aluminum composites (Al/Al2O3-MMC) by powder metallurgy method. Phys B Condens Matter 405:896–899. https://doi.org/10.1016/j.physb.2009.10.010
37. Jiang S, Wang R (2019) Grain size-dependent Mg/Si ratio effect on the microstructure and mechanical/electrical properties of Al-Mg-Si-Sc alloys. J Mater Sci Technol 35:1354–1363. https://doi.org/10.1016/j.jmst.2019.03.011
38. Prabhu TR (2017) Effects of ageing time on the mechanical and conductivity properties for various round bar diameters of AA 2219 Al alloy. Eng Sci Technol Int J 20:133–142. https://doi.org/10.1016/j.jestch.2016.06.003
39. Azimzadegan T, Serajzadeh S (2010) An investigation into microstructures and mechanical properties of AA7075-T6 during friction stir welding at relatively high rotational speeds. J Mater Eng Perform 19:1256–1263. https://doi.org/10.1007/s11665-010-9625-1
40. Liu Y, Deng C, Gong B, Bai Y (2019) Effects of heterogeneity and coarse secondary phases on mechanical properties of 7050-T7451 aluminum alloy friction stir welding joint. Mater Sci Eng A 764:138223. https://doi.org/10.1016/j.msea.2019.138223
41. Alpas AT, Zhang J (1992) Effect of SiC particulate reinforcement on the dry sliding wear of aluminium-silicon alloys (A356). Wear 155:83–104. https://doi.org/10.1016/0043-1648(92)90111-K
42. Chiker N, Benamor A, Hadji Y, Haddad A, Hakem M, Azzaz M, Sahraoui T, Hadji M (2020) Microstructure and tribological behavior of in situ TiC-Ni(Si,Ti) composites elaborated from Ni and Ti3SiC2 powders. J Mater Eng Perform 29:1995–2005. https://doi.org/10.1007/s11665-020-04710-3